JGR Space Physics

RESEARCH ARTICLE
10.1029/2021JA029492

# The Onset of a Substorm and the Mating Instability

**Gerhard Haerendel[1] and Harald Frey[2]**

[1]Max Planck Institute for Extraterrestrial Physics, Garching, Germany, [2]Space Sciences Laboratory, University of California, Berkeley, Berkeley, USA

**Key Points:**

- Growth phase arc brightening and instability and reconnection in the near-Earth tail are completely separate processes
- Auroral streamers may be low-entropy content bubbles with a flow channel attached and manifested by an Alfvénic arc
- Mating of two unconnected current sheets by a non-MHD process creates a channel for outflow of energy from the high-beta plasma layer

**Supporting Information:**

Supporting Information may be found in the online version of this article.

**Correspondence to:**

G. Haerendel,
hae@mpe.mpg.de

**Citation:**

Haerendel, G., & Frey, H. (2021). The onset of a substorm and the mating instability. *Journal of Geophysical Research: Space Physics*, *126*, e2021JA029492. https://doi.org/10.1029/2021JA029492

Received 29 APR 2021
Accepted 22 SEP 2021



**Abstract** The paper underlines the view that the appearance of beading and its nonlinear growth in the onset arc occurs independently from the onset of reconnection in the tail at about 20 $R_E$. Both events follow from an extreme thinning of the central current sheet of the tail at the end of the growth phase. Subsequently, we concentrate on the processes connected with the onset arc breakup. Its origin lies in the instability of a high-beta plasma layer building up at the outer boundary of the dipolar magnetosphere during the substorm growth phase, the growth phase arc (GPA) being the ionospheric trace. The observation of auroral streamers triggering the onset arc instability lets us analyze what is known about auroral streamers with strong support from high-resolution videos of two substorm onsets. We conclude that they may be low-entropy content bubbles with a balanced field-aligned current system, framing a flow channel. However, there are unresolved questions. The visible streamer is identified as an Alfvénic arc. In searching for a mechanism by which a streamer bubble lining up along the GPA can trigger the instability, we are led to the recognition that an entirely new non-MHD process must be at work. Taking also into account the surprising fact that the beads are moving oppositely to the convection in GPA and auroral streamer, we postulate the appearance of a new current system in the gap between the two. What happens can be described as the *mating of two current sheets,* which were completely separated before. It breaks the stability of the high-beta plasma layer and channels the release and conversion of free internal energy. For this reason, we name the process *mating instability*. A physical analysis of this process shows consistency with detailed features exhibited by the two videos

**Plain Language Summary** The substorm begins with two independent events of common origin. The first one is normally the brightening of the growth phase arc, which is the trace of a hot plasma layer forming at the inner border of the tail. The second one is due to flow bursts, emerging from reconnection in the tail, arriving at the inner edge of the tail, the very reason for the substorm. The common origin is the thinning of the tail current sheet due to the stretching by the solar wind. The paper is devoted to the understanding of the first event. As observed about 10 years ago, the brightening of the growth phase arc with beadlike structures and growth of instability is often triggered by a weak arc, an auroral streamer, arriving from high latitudes and lining up with the growth phase arc. The paper proposes that the trigger process involves the formation of a new current circuit between the two arcs by the mating of the neighboring current sheets, which involves a non-MHD process. It generates the sudden appearance and motion of the beads and constitutes a channel for the outflow of internal energy of the high-energy plasma.

## 1. Introduction

During a substorm, the energy accumulated in the tail is released and injected into the magnetosphere. The energy accumulation phase, the growth phase, begins with magnetic reconnection on the dayside leading to the transport of magnetic flux across the polar cap into the tail. Stretching and compressing of the tail field by the solar wind leads to thinning of the central plasma and current sheets. This process is accompanied by the transport of closed magnetic field from the near-Earth tail and nightside magnetosphere toward the morning and evening magnetopause. The equatorward motion of the southernmost auroral arc, the growth phase arc (GPA), is a consequence of that. At substorm onset, this or a nearby arc starts brightening and is followed within a few minutes by a poleward expansion of auroral activity proceeding in successive steps (Akasofu, 1964; Oguti, 1973; Sergeev et al., 2000). This definition of the *substorm onset* is identical with the one given by Akasofu (1964) under the designation “expansive phase”. He distinguished two stages of the onset, (a) sudden brightening and (b) rapid poleward expansion. He actually defined a third stage for the

substorm expansion. It applies to the expansive bulge reaching its most poleward location and the further west-and eastward expansion. This phase contains the further processing of the injected energy and is not the subject of this paper. Later research revealed that the rapid poleward expansion phase is due to the arrival of flow bursts or dipolarization events initiated by reconnection in the near-Earth tail (Angelopoulos et al., 2008; Runov et al., 2009; Sergeev et al., 2011), and the substorm current circuit is generated by flow braking or vortex formation near the inner edge of the tail (Birn et al., 1999; Shiokawa et al., 1997). Birn et al. (2004) and Birn and Hesse (2013) have elaborated on the vortex formation and associated current systems. Haerendel (2015b) has added another variant.

So far, we can consider the onset of a substorm as well understood. However, this is not the case with respect to the events at the inner edge of the tail. The initial brightening of the growth phase arc is characterized by the appearance of a fast moving wavy structure, so-called beads, which quickly develop into larger-scale bright folds, protrusions, or vortexes (Donovan et al., 2006; Dubyagin et al., 2003). Obviously, a nonlinear instability is proceeding, which has been commonly interpreted as a kind of ballooning instability (Derr et al., 2020; Kalmoni et al., 2015; Pritchett & Coroniti, 2010; Ohtani & Tamao, 1993; Roux et al., 1991; Voronkov et al., 1997). In recognition of these manifestations and interpretations of the initial brightening, we are using for it synonymously the terms "onset arc breakup" and "onset arc instability". An important new aspect was the observation by Nishimura et al. (2010) that the substorm in many cases appears to be triggered by an auroral streamer approaching the onset arc. This streamer was shown to originate out of the poleward boundary intensifications, PBIs, which probably are related to the distant neutral line, a phenomenon already well known by the work of Lyons et al. (2002) and Zesta et al. (2002). However, it is not known whether the brightening of the GPA or onset arc always needs to be triggered by an auroral streamer (Mende et al., 2011). The streamers are often sub-visual for an all sky since the early nineties camera.

Since the early nineties, many researchers have pursued the concept of the substorm being initiated by the instability at the inner edge of the tail (e.g., Dubyagin et al., 2003; Haerendel, 2010; Lui, 1991; Rae et al., 2009). While this kind of reasoning has largely disappeared from the discussion of the onset, the view is spreading that the events at the inner edge of the tail, the appearance of beading, and its nonlinear growth are independent of the substorm breakup and poleward expansion (Kalmoni et al., 2018; Lui, 2020; Nishimura et al., 2016). There is typically a waiting period of a few minutes between this brightening of the onset arc and the initiation of poleward expansion (Nishimura et al., 2016) or the arrival of the flow bursts with all the consequences (Haerendel, 2015b). What has remained as an unsolved mystery is the way the triggering of this process by the interaction with an auroral streamer might function.

This paper is focusing on the latter question. Before coming to the crucial process, we demonstrate the independence of the beading instability from the substorm breakup and poleward expansion by observations from an isolated substorm, the underlying common cause being the extreme thinning of the tail current sheet. The next step is a brief discussion of the accumulation of plasma energy at the outer boundary of the near-dipolar magnetosphere and the inner edge of the tail during the growth phase. In the following section, we summarize what is known about the nature of the pre-onset auroral streamers. We base the subsequent discussion of the physics of the trigger process on a careful analysis of two well-documented substorm onsets, one before, the other after magnetic midnight. The surprising fact that the beads are moving oppositely to the convection in the region before onset leads to the insight that a non-MHD process initiates the formation of a new current system in the gap between GPA and streamer. It enables instability and channels the dumping of the released energy and momentum. A detailed physical analysis of that process reveals consistency with the observations.

## 2. Independence of Beading Instability and Launching of Flow Bursts but Common Cause

A full satellite mission, Time History of Events and Macroscale Interactions during Substorms (THEMIS), has been devoted to the clarification of the question of whether reconnection in the tail may be triggered from processes at its inner edge, like current disruption, or whether the reverse is happening. The initial timing studies seemed to support initiation by reconnection in the near-Earth tail around 20 $R_E$ and consequential excitation of the auroral phenomena at the inner edge (Angelopoulos et al., 2008; Mende

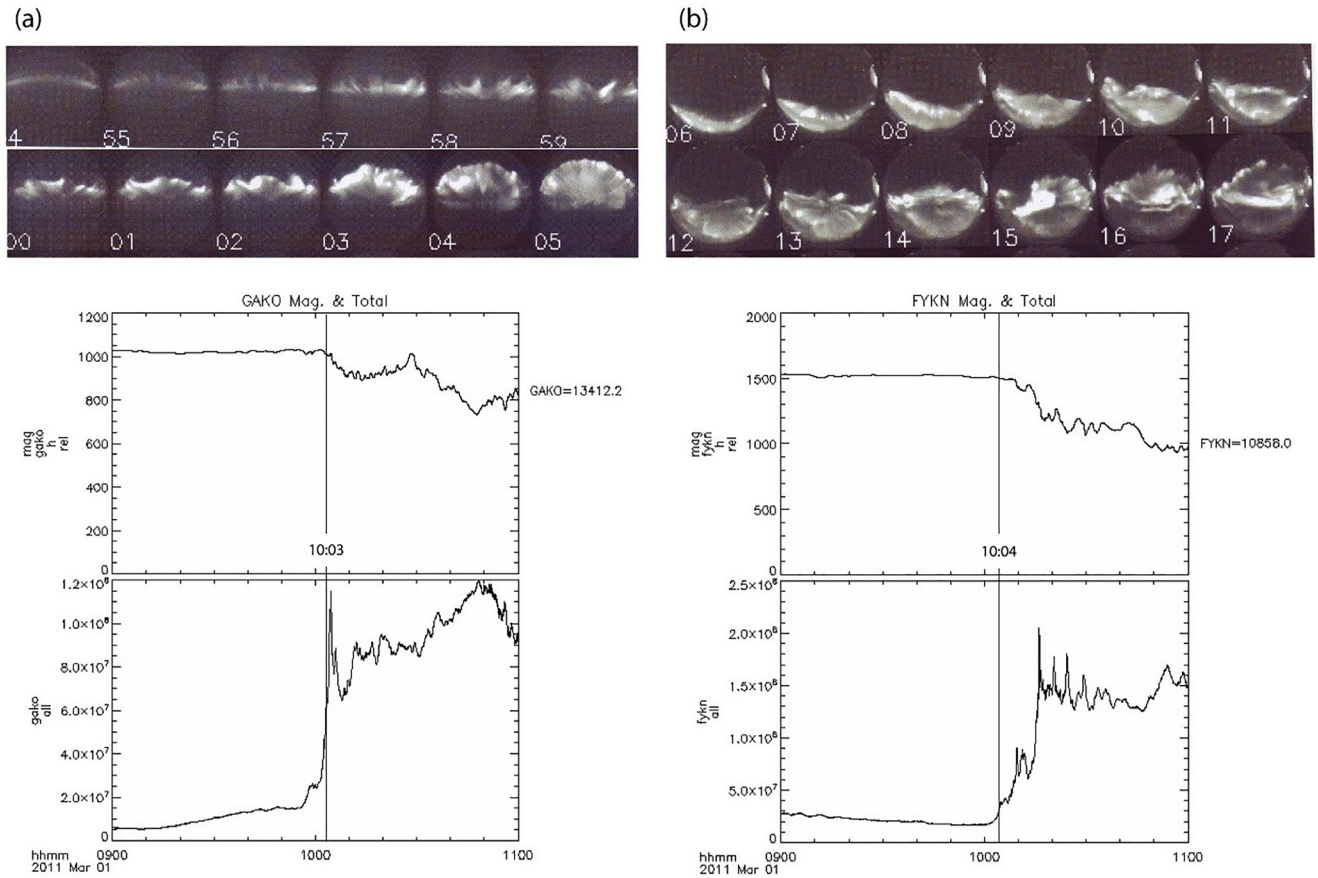


**Figure 1.** (a) (Upper panels left) 12 Minutes of substorm onset on March 1, 2011 seen from Gakona, AK, 62.4°N, 215°E. Appearance and nonlinear evolution of auroral beads starting at 09:54. At 10:03 new narrow structured arcs appear at the polar edge. They signal the arrival of flow bursts from reconnection site. (Lower left panels) Two hours of the H-component of the ground-based magnetic perturbation and (below) integrated brightness of all sky image. (b) (Right panels) Same as (a) with images for the continuing 12 min, H-component, and integrated brightness from Fort Yukon, AK, 66.6°N, 215°E. Sequential arrival of flow bursts and subsequent evolution.

et al., 2009; Sergeev et al., 2011). Concepts of substorm initiation from the inside had been promoted since the early nineties (e.g., Dubyagin et al., 2003; Haerendel, 2010; Lui, 1991; Rae et al., 2009). Nishimura et al. (2010) introduced a new aspect. Frequently, it seemed to be the arrival of an auroral streamer near the onset arc that triggered its sudden brightness increase and nonlinear development of structures (Mende et al., 2011; Nishimura et al., 2010). Somewhat later Nishimura et al. (2014) concluded that the interaction of pre-onset waves at the onset arc with earthward flows from downtail evolved into the substorm onset instability. It was not clear whether that meant a causal relation in the above sense. Haerendel (2015a) related the brightening of the onset arc to a current sheet avalanche of high beta plasma flows, which become abruptly stopped at the outer magnetospheric boundary. He regarded this event as independent from the launching of flow bursts at about 20 $R_E$ and both as due to an extreme thinning of the central current sheet and therefore nearly coincident within minutes.

Data from an isolated substorm on March 1, 2011 provide support for a common cause but the independent onset of the two events or better phases, that is, the brightening of the onset arc and the poleward expansion due to the arrival of flow bursts. Figure 1 contains all sky images from Gakona and Fort Yukon and the concurrent development of the ground magnetic perturbation and integral brightness. Figure 1a shows that beading starts in the Gakona area at 09:55 UT. For 9 min there is no indication of an electrojet flow in the magnetic data, although the brightening occurs nearly overhead. The aurora exhibits the typical morphology of a nonlinear growth from beading to protruding folds of increasing scale. At 10:04 at both stations, but better visible from Fort Yukon (Figure 1b), the brightness increases rapidly and the horizontal magnetic perturbation turns negative. The aurora shows a new element. Narrowly structured arcs appear

in successive poleward steps at the poleward edge of the auroral activity. Within about a minute, they turn into diffuse brightness on the equatorward side, while new narrow arcs appear poleward. This phase, which persists for the next 20 min, is a manifestation of the sequential arrival of several flow bursts. The poleward expansion is nothing else than the agglomeration of new magnetic flux carried by the flow bursts. Similar sequences of events can be found just by searching through the all-sky images from the THEMIS ground-based network. Narrow erratically structured arcs, signaling the arrival of flow bursts, have been explained by Haerendel (2015a, 2015b) as resulting from the formation of a stop layer, i.e., the abrupt stoppage of a high-beta plasma flow over an ion inertial length. There is a distinct difference between the auroral phenomena in the two phases. While the onset instability of eight minutes exhibits the rapidly growing release of energy stored in or near the growth phase arc, thus being an internal event, the subsequent phase is clear evidence for new energy and momentum arriving from downtail. During the latter phase, one can distinguish up to six successive steps led by stop layer arcs. This phase is fully consistent with the sequence of substorm injections and poleward expansions observed by Akasofu (1964), Oguti (1973), and Sergeev (2000). In conclusion, we maintain that there is no causal relation between reconnection downtail and the nonlinear brightenings of the onset arc. However, both processes are independently preconditioned by an extreme thinning of the central current sheet of the tail. In the case of the reconnection process, the role of thinning is obvious. Its role in the instability of the onset arc will emerge later. It should be added that the eight minutes wait for the arrival of flow bursts in the above-documented event is unusually long. Nishimura et al. (2016) found typically duration times of less than 200 s. Although not causally related, but preconditioned by the same process in the tail, Akasofu's (1964) combining the two phases as *Stage I* and *Stage II* of the "expansive phase" appears quite appropriate.

One may argue that a single event cannot be regarded as proof for general independence of flow burst launching and onset arc breakup. However, more and more investigations, such as Kalmoni et al. (2015), Nishimura et al. (2016), and Lui (2020) come to the same conclusions. With respect to the instability process as such, an inspection of the auroral images and theoretical work has strongly promoted the conviction that some sort of ballooning instability, preferentially related to shear flows, must be at work (Derr et al., 2020; Kalmoni et al., 2015; Ohtani & Tamao, 1993; Pritchett & Coroniti, 2010; Roux et al., 1991; Voronkov et al., 1997). Current disruption (Lui, 1991; Lui et al., 1990) or cross-field current instability (Kalmoni et al., 2015; Lui, 2020) have been proposed as alternate processes, while Haerendel (2010) interpreted the growing structures as resulting from the inflow from a collapsing current sheet. The above-presented evidence for an independent instability at the inner edge of the tail raises the question of the source of energy. This is addressed in the next section.

## 3. What Happens at the Inner Edge of the Tail During the Growth Phase?

Following reconnection of solar wind magnetic field with the terrestrial one at the dayside magnetopause, new magnetic flux is added to the tail, which becomes strongly stretched and compressed. As one of the consequences, a closed, but stretched magnetic field in the near-Earth tail is ejected earthward and transported toward the morning and evening magnetopauses (Coroniti & Kennel,, 1972). Thereby the tail plasma sheet and central current sheet become increasingly thinner while compressed plasma accumulates at the outer boundary of the magnetosphere. Kadokura et al. (2002) presented detailed evidence for the related earthward directed two-cell convection during the growth phase, which moves the equatorward arc of the auroral oval further equatorward (Akasofu, 1964). Crossing of the GPA by the Akebono spacecraft shows clearly the relation between the proton arc and a high-energy ion layer extending in energy well beyond 10 keV. Deehr and Lummerzheim (2001) and Samson et al. (1992) have traced the different components of hot ions, soft and energetic electrons of the growth phase arc. While the ions of up to and beyond 10 keV penetrate more deeply into the outer magnetosphere, it is the poleward flank of the GPA, dominated by lower-energy electrons, where the auroral breakup proceeds preferentially. An important detail is that the growth phase convection continues along the GPA, separating into a morning and evening arm. Consequently and shown in Figure 2, the poleward edge of the GPA is pervaded by upward currents on the evening side and downward currents on the morning side (Haerendel, 2010). This pattern has been reproduced in the simulation of the growth phase using the RCM-E model by Yang et al. (2013) and by using the same model also by Nishimura et al. (2016). This can give the impression that breakup on the morning

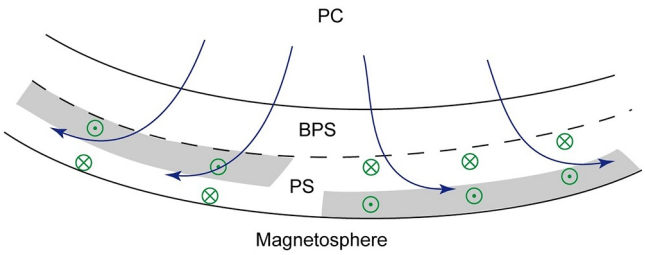


**Figure 2.** Polar cap convection into the growth phase arc dividing between evening and morning (after Haerendel [2010]). Current sources and sinks marked in green.

side is related to a new onset arc. Indeed, the onset arc just designates the location of the instability.

Baumjohann and Paschmann (1989) and Lui and Hamilton (1992), the first with the AMPTE/IRM, the second with the AMPTE/CCE, discovered the presence of high-beta plasma outside and inside the border of the near-dipolar magnetosphere on the nightside. Beta values of up to 10 and densities somewhat below 1 $cm^{-3}$ constitute a substantial source of energy, of course, dependent on geomagnetic activity. Haerendel (2010) postulated an outflow from the central current sheet as the source of the high-beta plasma. Yang et al. (2013) modeled the transport of plasma under compression from the near-tail toward the interface with the near-dipolar magnetosphere by using the Rice Convection Model, RCM-E, and obtained very high beta values. In their work on shear-flow interchange instability, Derr et al. (2020) show growth phase simulations with the RCM-E model clearly exhibiting beta values up to 40 in the central near-Earth plasma sheet. Coroniti and Pritchett (2014) related the quiet evening arc and in continuation the growth phase arc to the current and pressure distribution in the near-Earth tail. Irrespective of the detailed concepts pursued, it is important to realize that during the build-up of the high-beta plasma layer at the interface to the magnetosphere, the GPA remains stable for the whole growth phase, until instability is triggered. (The designation a 'layer' need not imply a concentrated sheet. It may extend radially by a few $R_E$.) This long-lasting stability must be attributed to an evolution of the plasma and field transport continuously maintaining stable gradients of the entropy contents, as is conserved in the modeling with the RCM-E. In view of this property of the growth phase, the nature of the auroral streamers and of the instability process, conspiring to break the stability, gains outstanding importance.

## 4. Pre-onset Auroral Streamers

### 4.1. Observations

Two types of auroral streamers have been identified. One class is encountered following substorm onset and poleward expansion and is a means for the distribution of energy inside the magnetosphere further to the initial penetration through the nightside magnetospheric boundary (Henderson et al., 1994; Nakamura et al., 1993; Rostoker et al., 1987). The other class, the one we are concerned with here, appears from the poleward boundary intensifications (PBI) prior to substorm onset and since the paper of Nishimura et al. (2010) are suspected to be crucial for triggering the intensification and nonlinear evolution of the GPA or onset arc. PBIs are commonly associated with the location of the distant neutral line or of the farthest extent of closed field lines before a substorm. Zesta et al. (2002) presented a broad overview of PBIs and the appearance of north-south or east-west oriented structures propagating equatorward (occasionally also poleward). They occur at all levels of geomagnetic activity, most frequently during the recovery phase of a substorm. The pre-substorm auroral streamers are thus a subset of the PBIs. Probably of great significance is a finding of Nishimura et al. (2014) with an isolated substorm that ionospheric flows propagated equatorward from the polar cap, crossed the PBI, and when reaching the growth phase arc, triggered the onset. However, this finding cannot yet be generalized.

The PBIs have mostly a life time of several minutes and a spatial extent over several degrees in longitude or latitude. This was shown by Zesta et al. (2002) by tracking the luminous structures by meridian scanning photometers into the field of view of all sky cameras. Perhaps most remarkable are their high proper motions of typically 600–800 m/s. This raises intriguing questions, in particular for east-west extending structures moving equatorward, namely how they avoid entanglement with the pre-existing magnetic field. The studies of Nishimura et al. (2010) included a great statistical set of north-south as well as east-west auroral streamers. In many cases, N-S oriented streamers turned into E-W arcs when getting close to the GPA. Mende et al. (2011) revisited a subset of the observations of Nishimura et al. (2010) and concluded that there was a class of largely different nature, namely E-W oriented thin arcs appearing before substorm onset, as for instance reported by Elphinstone et al. (1995) and Kornilova et al. (2006).

While earlier measurements of the association of streamers with balanced field-aligned current systems had already implied the presence of flow channels, the validity of the designation as "streamers" was confirmed by Gallardo-Lacourt et al. (2014) and Sergeev et al. (2004). The latter authors by using the SuperDARN radar determined the existence of N-S flow channels attached to the eastern flank of visible N-S arcs. The corresponding electric fields and related currents are consistent with the existence of balancing downward currents located to the east of the flow channel. A typical width was less than 100 km, while the visible length of a streamer could cover a few degrees in latitude. Furthermore, the flow channels were also found to be flanked by return flows on either side. The flows do not only suffer frictional losses to the lower ionosphere. The low-intensity rayed arcs indicate the existence of concentrated field-aligned currents sustaining parallel electric fields, either quasi-stationary or (most likely) transitory, and thus additional energy losses. Therefore, the flows must be driven along their paths by some renewable force. Buoyancy is a likely candidate. We return to this aspect in sub-section 4.3.

### 4.2. Two Types of Streamers?

More information about the nature of auroral streamers comes from higher resolution imaging and from accidental satellite crossings. However, so far not one case covered by simultaneous measurements of both types has been reported. Therefore, we have an unclear situation with respect to the nature of an arc identified as streamer. There may actually be two classes, those with mono-energetic electron spectra and those with diffuse spectra and strongly field-parallel distributions. These classes seem to be distinguished as well by their optical appearance. The first appear more or less as homogeneous bands, the latter show coarse and highly fluctuating rays, mostly with no clear sense of motion discernible. This clearly differs from the first class and strongly suggests the presence of kinetic Alfvén waves.

Close to an ideal coverage was the crossing of a three degrees wide streamer by the DMSP spacecraft on the southern hemisphere reported by Sergeev et al. (2004). Supported by Polar UVI observations from the conjugate northern hemisphere, the in situ drift meter and magnetic field data clearly reveal the existence of an inclined flow channel. The electron spectrum in the upward current sheet has a strong spectral peak at 4–10 keV but also a strong diffuse spectrum below 1 keV. The evidence for mono-energetic spectra remains ambiguous. The Polar UVI images show that a rather luminous streamer is separating from the PBI moving all the way toward the GPA. A similar event is contained in Figure 3 of (Haerendel et al., 2012). While the keogram from Ft. Simpson shows diffuse traces of the streamer, local imaging reveals the erratic ray nature of the streamer, however only after it had arrived at the polar boundary of the evening oval. The FAST data at that instant confirm the diffuse spectrum and focused electron fluxes typical for Alfvénic arcs. These examples demonstrate the difficulties to determine the true nature of auroral streamers from incomplete data sets.

Alfvénic arcs have been studied extensively by Chaston et al. (2003, 2006, 2008), Louarn et al. (1994), Stasiewicz et al. (2000), and Wahlund et al. (1994), without reference to the ray structure and dynamics. However, the observed or implied connections with electromagnetic fluctuations, vortex structure, and multiple reflections in the Alfvén resonator are consistent with their optical appearance. The main characteristics are the presence of strongly field-aligned electron fluxes, diffuse spectra, mostly below 1 keV, and transversely heated ions. They are associated with balanced field-aligned currents of tens of km widths and highly fluctuating electric and magnetic fields in the range of 1–10 kHz. Haerendel and Frey (2014) studied Alfvénic arcs at the polar border of the substorm bulge, where they seem to constitute a transitory stage for the penetration of energy from the tail into the magnetosphere. The erratic ray structure seems to be best associated with the energization by kinetic Alfvén waves somewhere in the topside ionosphere. An important effect of the presence of Alfvénic arcs is the erosion of the upper ionosphere. Chaston et al. (2008) have shown that turbulent cascades from MHD scales down to the electron skin depths are powering these arcs. This happens largely by scale breaking and multiple reflections inside the ionospheric Alfvén resonator. This has been confirmed by Haerendel and Frey (2014), who showed that as a consequence the arcs decouple effectively from the lower ionosphere.

Mende et al. (2003) presented a remarkable encounter of an Alfvénic arc at the border of the substorm bulge, which FAST crossed just one minute after onset. It had all the above characteristics of an Alfvénic arc, like balanced field-aligned currents, diffuse spectra, and strongly downward focused electron fluxes.

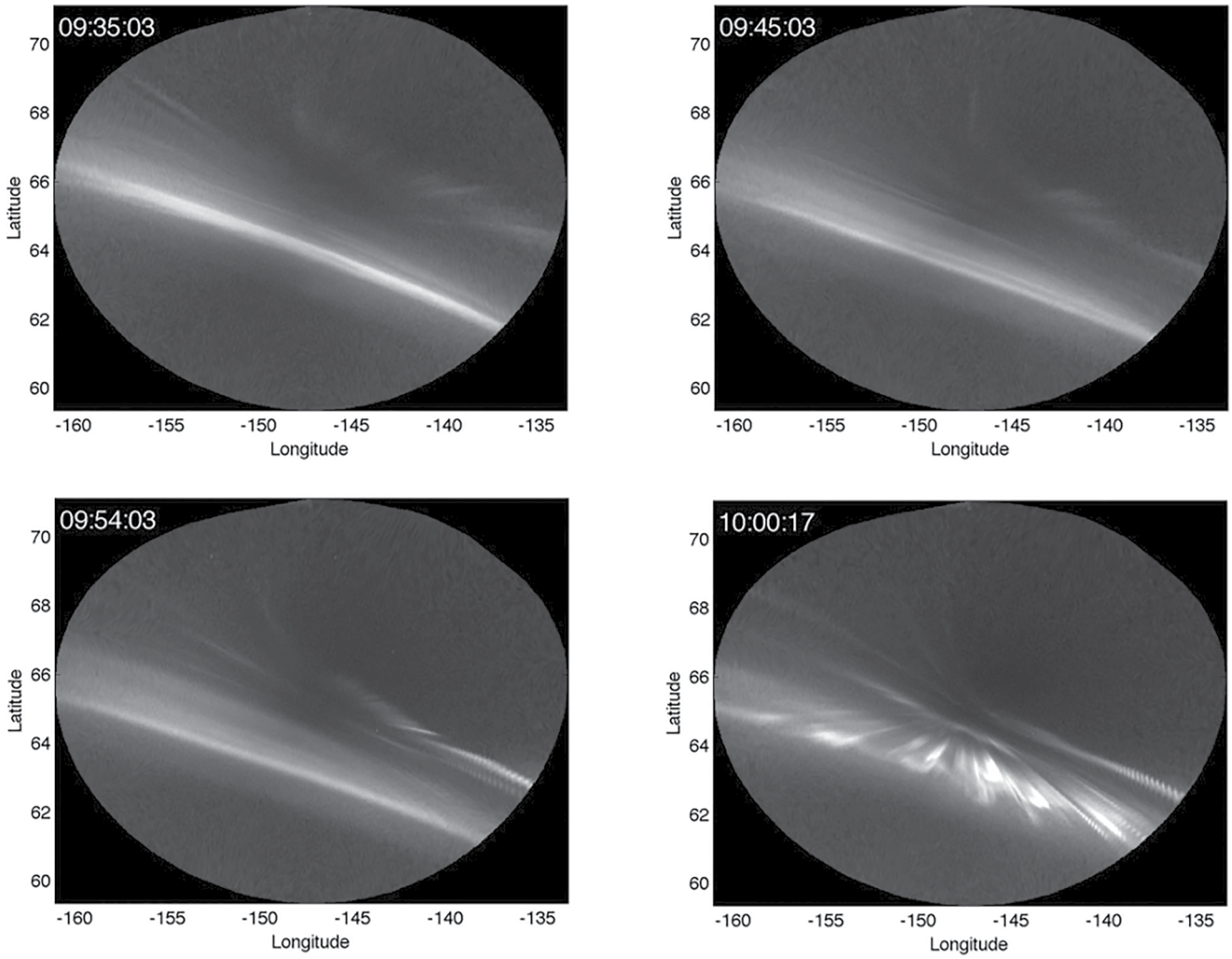


**Figure 3.** Pre-onset arcs approaching the growth phase arc on March 1, 2008 at 09:35-10:00 UT. A new arc appears at 09:54 UT.

Unfortunately, there was no optical coverage. It may have been an auroral streamer before substorm onset. During the two minutes before this crossing, it appears from Figure 3 of that paper that three streamers may have been encountered further poleward. The magnetic perturbations showed that like the arc at the border, all three were framed by currents implying eastward drifts. These events happened shortly before magnetic midnight.

Magnetic local time may be important information because our next example showing auroral streamers indicates clearly ray motions in the westward direction at more than one hour before magnetic midnight. We present this event as Supporting Information 1 by a highly time-resolved video of a substorm on 01 March 2011 over central Alaska. It is the same event as that underlying in Figure 1 and quite similar to the event published by Kornilova et al. (2006). A rayed E-W arc is already visible 20 min before the onset of beading at 09:55 UT at about 1.5° further north (Figure 3). It moves slowly with about 150 m/s toward the growth phase arc, which is still moving equatorward and thinning. The motion of the rays is clearly westward, indicating that the arc is embedded in a westward flow. According to the discussions in Section 3 and Figure 2, the flow along the growth phase arc must also have been directed westward at 1:20 h before magnetic midnight. Although we have no magnetic data, we conclude that this arc was also associated with balanced field-aligned currents, upward on the poleward side and downward on the equatorward side. This is going to be important for our later reasoning. Unfortunately, this is the only data set we have on E-W arcs with high time resolution.

In conclusion, we do have evidence for erratically rayed arcs being of Alfvénic nature. An arc qualifying as an E-W arc or auroral streamer and exhibiting such rayed structure is most likely an Alfvénic arc. However, we cannot exclude the existence of auroral streamers with mono-energetic electron spectra (Forsyth et al., 2020; Sergeev et al., 2004). It remains unclear whether the spectral characteristics differ with the optical appearance and whether the E-W arcs are at all connected with flow channels The shortage of undisputable events with simultaneous optical, particle, and field measurements is deplorable.

### 4.3. Streamers as Low-entropy Content Bubbles

From this summary of observed and derived properties of Alfvénic arcs and a few auroral streamers, we conclude that the overarching structure of E-W streamers must be alike that of N-S streamers, which were proven to be attached to flow channels. Zesta et al. (2002) presented cases of streamers separating from the PBI location above about 70° MLAT with an overall speed of about 500 m/s. The extension over several degrees of longitude raises the question asked already above: What keeps them moving equatorward and how do they interact with the established convection and magnetic field pattern? Embedded arcs have a proper motion of typically 100–200 m/s (Frey et al., 1996; Haerendel et al., 1993). This is another argument for not identifying auroral streamers with this class of arcs. What remains is low entropy content bubbles. Pontius and Wolf (1990) explained transient flux tubes in the tail as bubbles of reduced entropy content. A large number of publications have appeared exploiting this concept (e.g., Chen & Wolf, 1993; Kauristie et al., 2000; Nakamura et al., 2001; Sergeev et al., 1993). Birn et al. (2004, 1999) have adopted the bubble concept for MHD simulations of the flow bursts and dipolarization events. Nakamura et al. (2001) argued that also auroral streamers have the characteristics of bubbles. Sergeev et al. (2012) regarded the question of substorm preconditioning by auroral streamers and breakup onset by the arrival of flow bursts as unresolved. Yang et al. (2014) simulated auroral streamers with the Rice Convection Model RCM-E as thin arcs arising from a plasma sheet bubble. It is interesting that the bubble splits at the inner edge of the tail into the evening and morning-side lower-entropy–content regions. On the evening side, the field-aligned current pattern resembles the E-W arcs discussed in Section 4.1. On the morning side, the reverse pattern appears. On both sides, the split bubble interacts with and enhances the pre-existing current structure.

A way of understanding what drives a bubble refers to the force exerted by the environment on the interior. As the internal plasma pressure is reduced and the magnetic pressure is enhanced, a fraction of the magnetic force is not supported by the internal pressure gradient. This is what accelerates the bubble. In this view, the generator of the field-aligned currents is located in the interior of the bubble and carried by the magnetic gradient and curvature currents of the excess internal field, opposite to the external tail current. If the acceleration is slow or absent, field-aligned currents do exist. They apply the work done on the bubble by the environment where they are closing, for the streamers obviously in the ionosphere. The internal energy and entropy contents are adjusted to the changing environment on the path toward the Earth. In the simulation of a (narrow) bubble, Birn et al. (2004) have shown how the environment is forced to flow around the bubble, quite consistent with the findings of Gallardo-Lacourt et al. (2014).

Forsyth et al. (2020) in a comprehensive review of present knowledge on auroral streamers support the view that the growth-phase streamers have an origin at a distant neutral line and thus belong to a wider class of reconnection flow related auroral brightenings. In so far they would fulfill the property of low-entropy content bubbles similar to the BBFs. However, too little is quantitatively known about the streamers in order to prove that buoyancy can provide a sufficiently strong force on them to do the necessary work on the environment. The bubble nature remains a conjecture.

There are, however, problems with the identification of auroral streamers with low-entropy bubbles. First, when separating from the PBI the streamers are quite luminous, in particular in the 6,300 Å oxygen line. Combined with the indications of being loaded with accelerated ionospheric matter (Nishimura et al., 2014) this suggests considerable mass content. Since the greatest fraction of the flux tube of a streamer must be embedded in the low-density tail lobe, it is hard to see how it can fulfill the criterion of a bubble. Secondly, what causes conceptual problems is the evolution of the internal flow channel as the bubble moves from the open/closed boundary toward the growth phase arc. Do the flows interchange plasma and field with the environment in this way and how can they maintain their low-entropy content nature? Taken together, these problems accumulate in the question: What drives the motion of the streamer flux tubes and supplies

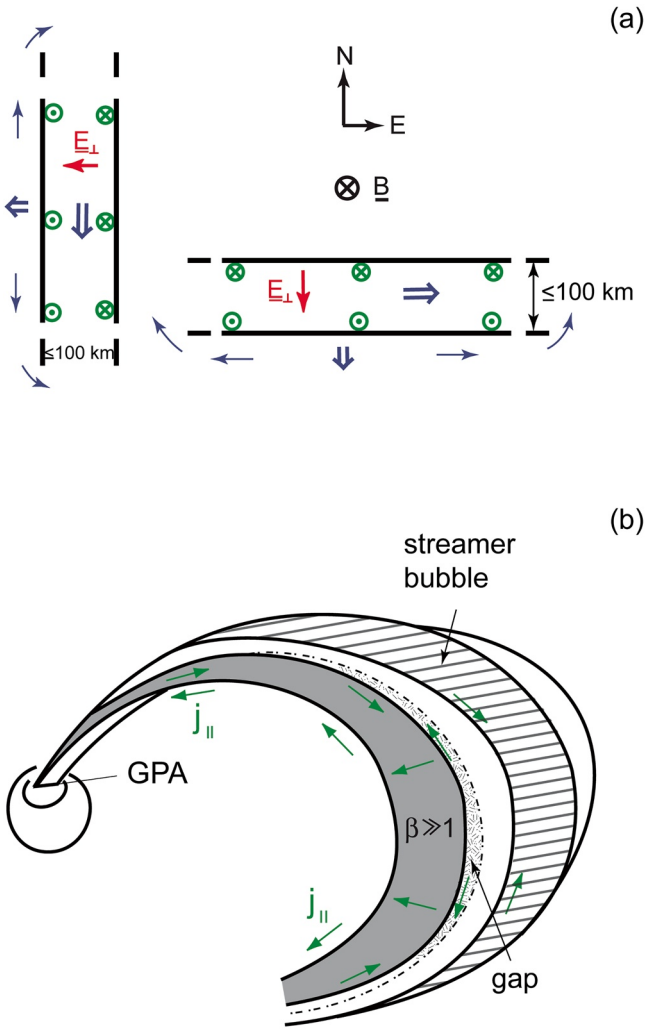


**Figure 4.** (a) Ground projection of field-aligned currents (green circles), electric fields (red arrows), and flows and motions (blue arrows); (b) E–W streamer bubble attaching to the high-beta plasma layer.

the energy carried away by the Alfvénic arcs and consumed by electron acceleration and ionospheric friction? Although the most likely driver is magnetic buoyancy, this clearly needs deeper considerations and studies exceeding the scope of this paper. We put these problems aside and regard the auroral streamers as conjugate flux tubes with flow channels, N-S or E-W, attached as sketched in Figure 4a. Figure 4b shows the related flux tube embracing the high-beta plasma layer.

## 5. Bead Motions and the Trigger Situation

### 5.1. Bead Motions

We have argued that the substorm onset consists of two independent events, the release of energy from energy storage at the inner edge of the tail and the arrival of flow bursts after reconnection in the mid-tail. The first event is suspected to arise from an instability triggered by contact with an auroral streamer. While the instability and the associated release of internal energy occur high up in the magnetosphere, the evidence is derived from the energy deposited in the ionosphere to form so-called beads, moving wavelike structures growing nonlinearly into coalescent protrusions, folds, and vortices. Kalmoni et al. (2017) have shown that over 90% of the onset arcs show beads prior to the instability with scales of 30–50 km. The motions of the beads, typically 2–3 km/s, can be eastward or westward. Observations presented by Dubyagin et al. (2003), Haerendel (2015a), Kalmoni et al. (2018), Kataoka et al. (2011), Liang et al. (2005), Rae et al. (2009), and Shiokawa et al. (2009) show mostly eastward motions of beads and coarser structures. However, Sakaguchi et al. (2009) and Nishimura et al. (2016), from a large set of substorms onsets, found westward, bi-directional, and eastward motions, the latter clearly dominating. So far no clear ordering by direction has been found and no convincing interpretation of these motions. Whether arriving from east or west may depend on where in longitude the streamers are located in the above-mentioned polar cap flow. Nishimura et al. (2016) found a tendency for the direction of the bead motions to be westward or eastward depending on the onset location of the substorm being to the west or east of the minimum latitude of the growth phase arc. Onsets close to the minimum latitude point tend to be bidirectional. However, there is a great scatter in the relevant data. Kalmoni et al. (2018) demonstrate that the beads carry the signature of kinetic Alfvén waves launched in a high-beta plasma. Sorathia et al. (2020) found in global MHD simulations of the growth phase a self-consistent formation of low-entropy content bubbles due to ballooning-interchange instability at the tailward border of a high-entropy (high-beta) region in the outer magnetosphere. The ionospheric counterparts of the bubbles, the beads, move either duskward (premidnight) or dawnward (postmidnight) with speeds of order 10 km/s in the magnetosphere caused by the MHD stresses. These velocities are by one order of magnitude below those implied by the beading speeds observed by Nishimura et al. (2016) and Kalmoni et al. (2018) for the substorm onset when projected to the equator.

The fact that the growth phase arc has no structure while moving equatorward and becoming thinner and, after this motion has come to a stop, suddenly breaks into beading and nonlinear structures, strongly suggests the action of a trigger. The challenge is now to find mechanisms by which streamers or, specifically, pre-onset arcs, as defined by Mende et al. (2011), interact with the growth phase arc or, how a bubble would interact with the high-beta plasma layer. A difficulty is that often no potential trigger is observed at all or, when identified, it is hard to determine from the images how close the contact actually has been with the growth phase arc.

### 5.2. Two Well-Resolved Onset Events

The first event is the onset of the isolated substorm of March 1, 2011 with onset at Gakona a little less than 1 h before magnetic midnight. It has already been covered in Section 2 and Figures 1 and 3. In addition to the superposed all sky images from Gakona and Ft. Yukon (Supporting Information 1) we make use of an all sky video taken at Poker Flat (65,1°N, 212.6°E) and graciously supplied by Josh Semeter and Don Hampton (see also Supporting Information 1). The three stations, Gakona, Ft. Yukon, and Poker Flat, form a triangle with Poker Flat being farthest to the west and by latitude just in the middle of that of the two first stations. The FOVs of all three all sky cameras have strong overlaps.

The two traces of integrated brightness at GAKO and FYKN are shown in Figure 1, nicely reflecting the equatorward drift of the GPA after the onset of the growth phase at about 09:15 UT. While the brightness increases at the southern station, it becomes weaker at the northern station. The onset of beading at about 09:54 UT is best seen at the southern station, where the GPA appears only slightly poleward of the station (see Figure 1a). The high temporal resolution of the Poker Flat and Gakona videos show the first appearance of the beads at 09:54:50 UT. Only 30 s later, the beads have already quite pronounced amplitudes, suggesting a linear growth rate of less than 30 s. The appearance of the beads begins at the eastern edge of the visible GPA and proceeds quickly westward, while the phase velocity of the beads is eastward from the outset. This eastward motion presents a conundrum, as all other discernable motions in GPA and poleward arcs are directed westward (see below). After two minutes, the nonlinear structure with folds forming is well discernible. The eastward motions persist. During the next few minutes, large-amplitude protrusions and curls develop under strongly increasing brightness. Most important is that while the brightness is spreading westward, the observed phase velocities of the structures are eastward. Therefore, if one covered the event only by low-resolution imaging, one would probably observe apparent westward motions. As exhibited in Figure 1, the beading phase becomes overarched by the arrival of the first flow burst at 10:04 UT.

Taking a step backward to the growth phase starting at 09:15 UT, we see the GPA structured by longitudinal bands, which originate from the low-altitude edge and move upward within a few 100 msec. This is nothing else than the expression of the well-known field-aligned electron bursts (Arnoldy et al., 1999; Dahlgren et al., 2013; Ivchenko et al., 1999). By 09:46 UT this energy bunching of the electron acceleration has vanished, the GPA height structure is smooth, but one can discern the westward motion of very faint structures. The brightness has decreased and the arc looks thinner than before. By 09:54UT, the GPA has reached its southernmost location, and the beading sets in. Most important for the objectives of this paper is the equatorward progression of the erratically structured E-W pre-onset arc or streamer, which is well visible after 09:30 UT. It approaches more and more GPA and by 09:54:38 UT the lower edges of GPA and this arc are separated by a gap of about 250 km.

At this point, the importance of the extreme thinning of the central current sheet comes into play. Obviously, the supply of hot plasma to the high-beta plasma layer is exhausted. This must-have consequences on the growth phase arc. What comes to mind is the observation of Pellinen and Heikkila (1978) of a fading of the GPA a few minutes before breakup. No clear explanation has been offered for this phenomenon. Baumjohann et al. (1981) found that the equivalent current decreased during this interval, while the electric field remained unchanged. This is consistent with what our videos of 01 March 2011 (see Supporting Information 1) show: The arc is seemingly thinning and dimming. It seems as if a diffuse arc is splitting from the poleward edge of the arc starting about six minutes before the onset of beading, while the gap toward the E-W arc is narrowing. Without measurements of the precipitation rate and spectra, it is hard to assess what is happening.

The most important observation in pursuance of the trigger mechanism is the appearance of a new thin arc in the gap between the E-W pre-onset arc and GPA at 09:48 UT. Six minutes later, by the time of appearance of the beads, bright rays along the trace of this arc begin to emerge from the eastern edge of the FoV and expand quickly westwards, similar to what is observed with the growth and brightening of the beads. However, contrary to the beads, the rays are moving quickly westwards. The same is true for the rays of the E-W arc. Most significant is the development of the separation between GPA and the two arcs. As measured at the longitude of −145°, the equatorward speed of the GPA is about 105 m/s, until it stops at 62.8° geographic latitude at about 09:50 UT, while the E-W arc moves twice as fast with 220 m/s. Therefore, the gap between

the two arcs is narrowing but still about 250 km at beading onset. At this time, the new arc is north of the GPA by about 170 km at −145°, but already as close as 80 km at a longitude of −140 km. As this arc expands westwards, the gap with the GPA narrows.

The event on March 1, 2011 can be characterized by four observations: The appearance of a new arc in the gap between GPA and E-W arc shortly before onset of beading, its westward progression, the decreasing separation from the GPA, and the motion of the beads opposing the ray motions in the E-W arc and the new arc. Probably also the convection within the GPA was directed westward (see Section 3 and Figure 2). No doubt, the instability of the high-beta plasma layer must be intimately related to these facts. Both the fast rise time of the beads and the narrow gap hint in the same direction, a non-MHD process must be at work. For instance, a shear-flow interchange instability like proposed by Derr et al. (2020) or the ballooning-interchange instability of Sorathia et al. (2020), both involving flux tubes, would have growth times of at least twice the Alfvénic propagation time to the ionosphere, that is, more than one minute. As suggested by Kalmoni et al. (2015), Nishimura et al. (2016), and in the earlier literature (see Section 2), it must be some sort of kinetic ballooning instability, but proceeding locally in the hot plasma layer. The main question is: Why does the instability start only when close contact with a new arc is established and not earlier? The spatial scales of the hot plasma distribution are way too large for inciting local instabilities. Another type of short-scale change is required. It must reside in the electromagnetic structure. Here the gap comes into play. The westward progression and ray motions of the new arc imply the association with a poleward electric field and a dual current sheet, upward on the poleward side and downward on the equatorward side, the same sequence as inside the GPA. This conclusion, not yet supported by any in situ measurements, is critical for the following arguments. It also means that the quoted gap of only 80 km on the eastern edge of the new arc must house the downward current sheet. We are talking about a gap of less than 40 km between the two neighboring current systems. Projected up into the hot plasma layer, the distance to be bridged for an interaction of the two current systems may well be of the order of the ion gyroradius. In the next section, we will demonstrate that the mating of the two neighboring current systems opens a path for the instability to proceed. We, therefore, designate this process as *mating instability*. The trigger is then the appearance of a current system at a sufficiently close distance to the GPA.

Two questions arise from these observations and conclusions: What is the origin of the new arc before beading onset, and what enables this arc to approach the outer current sheet of the GPA until separated only by a gap of the order of an ion gyroradius? While we have assumed that the equatorward propagation of the E-W arc is most likely owed to its bubble nature, i.e., driven by the buoyancy force, we must look for another process. We have to take into account that the new arc appears from the east and intrudes into the gap between the E-W arc and GPA. It is therefore tempting to relate it to either one of the two pre-existing arcs, the E-W arc or the GPA. Unfortunately, the motions are fast and the contrast between the various structures is not high enough to draw definite conclusions. In any case, the westward growth of the new arc with about the same speed as the onset of beads in the GPA suggests that the proposed mating does not happen between the GPA and an already existing new arc, but progresses from the eastern edge along the GPA. In other words, the current system related to the new arc is unzipping the magnetic field pervaded by the upward current of the GPA. As we will discuss below, the new arc must have a substantially lower beta than the GPA. These are far-reaching deductions, raising more questions than answering the two questions raised above.

Before we turn to the physics of the envisioned trigger process, we have a look at the other example of a well-documented onset of the beading instability, which contrary to the previous example occurred at a later local time. It is the breakup event of February 29, 2008, shown in Figure 1 of (Mende et al., 2011) and is here presented as a video combining all-sky images from FSMI, ATHA, and TPAS (Figure 6 and Supporting Information 1). At the beginning of the short sequence, at 08:21:00 UT, a streamer is visible extending southward from the aurora at FSMI toward the growth phase arc at ATHA and turning east toward TPAS aligning with the growth phase arc. The situation is much more complex than our first example, which belonged to an isolated substorm. During the following 90 s, a brightening is running from FSMI along the streamer. At 08:22:27 UT beading starts with phase velocity being directed westward. As in the first event, the activation of the streamer proceeds opposite to the motion of the beads. This relatively small event took place at 01:20 MLT. At such local time, the convection inside the GPA as well as poleward of it should be

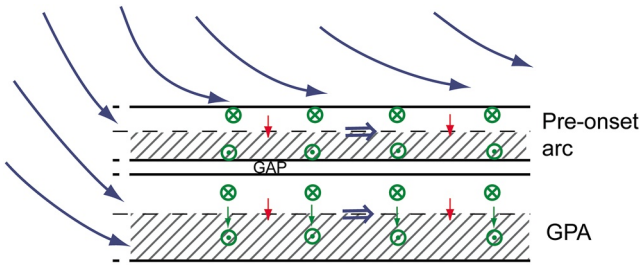


**Figure 5.** Field-aligned current foot prints for the situation shown in Figure 6.

directed eastward. This is also what the streamer exhibits. However, we have the same puzzling situation as in our first event, the beads move oppositely to the prevailing motions of the environment.

The all-sky images show that there is a dark gap between the beads and the GPA. That is no surprise. According to the current distribution in the GPA after midnight (Figure 2), the dark gap is the trace of the downward currents emerging from the poleward edge of the high-beta plasma layer, as demonstrated by the cartoon shown in Figure 5. It is the same situation as discussed by Dubyagin et al. (2003). The dark gap coincides with the so-called isotropic boundary location (Sergeev et al., 1993) or the b2i boundary in DMSP observations (Newell et al., 1996), indicating the outward limit of the adiabatic proton motion and the inward limit of strong non-adiabatic pitch-angle scattering of the protons. The instability develops, as in our first example, in the visible upward current region, which in this case belongs to the streamer. When the beads appear (at 08:22:27 UT), they run along the streamer arc. However, and this is important when the large protrusions develop, they extend into the dark gap of the downward currents of the GPA. Figure 6 and the video of the Supporting Information 1 show this very clearly. This is opposite to what happened on the evening side, where the protrusions expanded poleward. Unfortunately, neither the spatial resolution nor the brightness contrast of the streamer is sufficient to resolve the gap the same way as for the first event. On the other hand, there is another dynamic feature that both events have in common. Large-amplitude protrusions initially tend to extend with an inclination in the direction of the pre-existing convection, until suddenly turning in the clockwise sense (viewed along B) into the flow direction of the beads. The great question is again: Why do the beads move westward?

## 6. The Working of the Mating Instability

It is the appearance of a new arc in the gap between GPA and the E-W pre-onset arc that leads to the onset of the instability in our event #1. Obviously, the greater proximity of the new arc is decisive. Furthermore, in both events, the beads appear in the respective upward current sheet, of either the GPA or the adjacent streamer and extend into the gap between the two current systems. This suggests that the clue to the onset of the instability must reside in that gap, which is shown in Figure 4b. The opposing motions of beads and environment must be the result of something new happening in that gap. A new driver must appear. The obvious candidate is a process exploiting the free energy stored in the high-beta plasma. If the gap has narrowed down to a width of the order of $c/\omega_{pi}$ or, better, $R_{gi}$, the high-energy ions, not being magnetized over such scales, could bridge the gap to the new arc or streamer. Owing to the opposing directions of the field-aligned currents of the two neighboring current sheets, the hot ions would be neutralized by the electrons from the downward current along the neighboring flux tube. The pressure gradient would be the generator force acting in the poleward direction. As a result, a bridging current can flow across the gap, that is, in the direction opposite to the generator currents of the neighboring current systems. This way a new current generator is born which drives additional field-aligned currents in the adjacent sheets. Figure 7 displays field-aligned and bridging currents in a meridian plane for the situation of the first event.

The appearance of a new generator launches electromagnetic perturbations propagating in longitude and along B. An electric induction field arises which opposes the flow of the bridging current. Bridging means that the respective upward current is connected with the respective downward current across the gap. This process is what we designate with the word “mating”. With the ions not being magnetized, a longitudinal Hall current flows with the electrons moving in the direction manifested by the beads. Here we have the origin of the opposing bead motion. As we will see, it is the Hall current, which serves as a source of small-scale field-aligned current systems or better kinetic Alfvén waves. They carry the energy derived from the internal energy of the ions toward the ionosphere and generate the beads. The essential step in this chain of events is the *mating of two neighboring current sheets*. It establishes a path for shedding the internal energy of the high-beta plasma layer and is thus the origin of what can be rightly called *mating instability*. The non-MHD processes underlying the current sheet mating, i.e., the cooperation of ion diffusion, field-aligned

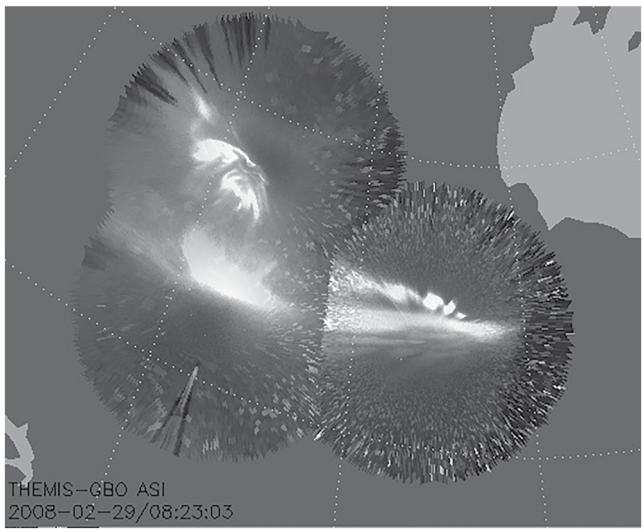


**Figure 6.** Westward moving nonlinear beads with protrusions extending into the downward current region of the growth phase arc.

currents, and Hall currents, is quite similar to what happens in the ion diffusion region of collision-free reconnection.

At this point, we have to check whether the assumed mating process can be quantitatively supported by the scales mapped from the gaps observed in the ionosphere to the high-beta source region. Unfortunately, the gaps are normally hidden in the observed brightness distributions of GPA and streamer or E-W arc. The only reliable data set available to us is the video of the 01 March 2011 onset, in particular the coverage from Poker Flat (Supporting Information 1). As analyzed in Section 5, the gap with the new arc is no more than 40 km wide. A typical scale for the proton gyroradius can be derived from the values of the plasma beta, the density, and the mean energy of the dominant ions. According to Baumjohann et al. (1989) and Lui and Hamilton (1992) the beta can range up to 10 near the equator. Using the conservative value of 4, a density of 0.8 $cm^{-3}$, and average proton energy of 5 keV, yields a magnetic field strength of 20 nT and a gyroradius of 510 km. Comparison of the magnetic field strengths in the ionosphere and near the equator suggests a mapping factor of about 40. Thus the gap would map into less than 1,600 km, perhaps substantially less. In view of the inherent uncertainties, we can regard these numbers as supporting the presence of kinetic proton scales comparable with the separation of the neighboring current systems.

The physical situation of the mating of current sheets is this: As the current system of the new arc is progressing along the high-beta plasma layer, there is initially an equilibrium of forces, essentially between the magnetic pressure force of the E-W arc and the pressure force of the high-beta plasma. In reality, there will be a less dramatic contrast. As perturbations arise, that side will win over the other, which carries the upward currents. The reason is that this current continues into the bridging current, which is the site of the primary conversion of the internal energy of the high-energy ions into electromagnetic energy. The bridging currents act as generators of field-aligned currents via the divergences of the Hall currents flowing along the gap. These currents or better the associated magnetic tensions transport energy and momentum from the hot plasma toward the ionosphere. For the configuration of our first event, this is shown in the cartoon of Figure 8 a, contrary to Figure 7, in the equatorial plane. Here, the currents are represented by green arrows and the electric field by red arrows. A Hall current starts flowing along the gap (Figure 8a). However, because of charge neutrality, the Hall current cannot carry more electrons along the gap than balanced by ions crossing into it. This leads to the structuring of the density along the gap, on the same scale as across the gap, namely about $R_{gi}$ (Figure 8b). This argument resembles the one used in the definition of the stop layer discussed in the study by Haerendel (2015a). The growing density perturbations generate secondary sources and sinks of field-aligned currents, which will propagate as kinetic Alfvén waves toward the ionosphere. The deposition of the energy they carry in the ionosphere is the origin of the beads. The scales are consistent with the 30–60 km observed at the first appearance of the beads (e.g., Sakaguchi et al., 2009). The reason for their direction of motion lies in the electric field across the gap.

It is very tempting to identify the observations of the FAST spacecraft when traversing the breakup arc, contained in Figure 3 of the already quoted paper by Mende et al. (2003), with an ongoing mating instability at one minute after substorm onset. The magnetic perturbations agree perfectly with the current configurations in Figures 7 and 8. The electron distributions match those of Alfvénic arcs, and the ion spectra show the existence of a strong population with energies well above 10 keV, with the arc located at its poleward edge.

Numerical simulations would be the suited tool to follow the further development of the mating instability. However, a simple way of clarifying the connection between the forces and motions is to look at the instantaneous force balances and current flows of an already evolved periodic density structure along the poleward plasma gradient. This is attempted in the cartoons of Figures 9 and 10, in which we try to illustrate, for both events respectively, the current and field situations in a quasi 3-D presentation, in a meridian plane, in the equatorial plane, and as a flux tube. The real situation of a smooth pressure gradient is

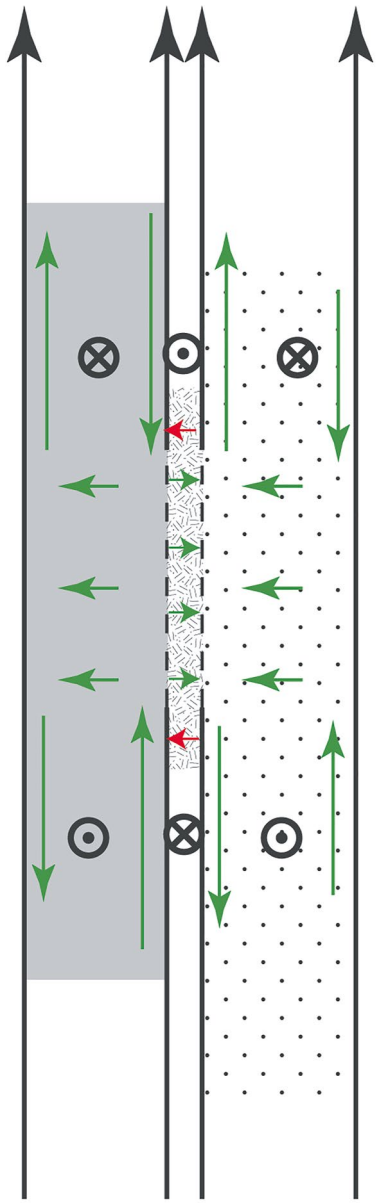

**Figure 7.** Currents (green) and electric fields (red arrows) of the neighboring current circuits of growth phase arc and streamer shown in a meridional plane of the evening sector across the equator. The black circles indicate the related perturbation fields.

deliberately represented by a high-beta region on the earthward side in contact with a low-beta region on the outward side. As the beads are developing into nonlinear protrusions, the combined action of the initially generated induction field across the gap with the small-scale tangential fields at the sources of the kinetic Alfvén waves leads to a progression of the structures opposite to the Hall current. In the situation of Figure 9 for the evening side, the grad $p_i$ force wins over the grad $p_B$ force and determines the direction of growth of the perturbations. The hot plasma is pushed poleward, in the sense of the pressure force, and loses energy doing work against the magnetic pressure force. The pressure minima move somewhat earthward because of the conservation of the magnetic flux. In the cartoon, the tangential components of the electric fields seem to be equal but with opposite signs, because we look only at the longitudinal motions. In reality, there is a net force driving poleward.

What is the nature of the source currents of the kinetic Alfvén waves? In the hot plasma, it is the Hall current. On the side of the streamer flux tube, it is the magnetic gradient current (the curvature current is negligible). In both cases, the internal energy of the plasma is being reduced. As shown in Figure 10, for the morning side, currents and electric fields are reversed. Here, the magnetic pressure force does work against the plasma pressure. In the low left-hand corner of the cartoon, one can see the two forces, $-\nabla p_i$, and $-\nabla p_B$, acting against each other at the border of the last protrusion, shown by gray shading. Here the magnetic gradient force from the new arc side wins. This is shown by the direction of the magnetic gradient current (green arrow), as well as by the tangential electric field (red arrow). As a result, the protrusion is being pushed westwards from its rear side. The leading edge, shown at the next protrusion to the right (white shaded), has the boundary current and electric field reversed. Here, the pressure gradient wins.

In the two latter cartoons, we have ignored the instability aspect. In reality, the longitudinal components of the electric fields (see also Figure 8b) do not balance each other. The component of the winning side will be a bit larger than that of the other side. For the evening situation, this applies to the eastward component, for the morning side it applies to the westward component. On the evening side, the net displacement of the nonlinear phase is directed outward. On the morning side, it is directed inward. In both cases, it is the radial momentum of the winning side, which is carried earthward by the kinetic Alfvén waves. As we have seen, the two analyzed substorm events support this conclusion.

The above-used argumentation, illustrated with the two cartoons, is resting on basic physical relations. We want to show that the onset arc brightening is strictly not instability of the hot plasma layer itself. It needs a configurational change. The unaffected hot-plasma distribution is probably smooth, for instance as derived by Dubyagin et al. (2003) or in the simulations of Yang et al. (2013) and Sorathia et al. (2020). Such distributions may be ballooning-interchange unstable, as has been shown by the latter authors. However, the spatial, that is, beading, scales would be larger and the growth rates substantially lower. The beading instability is thus not caused by the setup of strong density gradients, but by the appearance of a discontinuity in the current flow along B. The proposed name, *mating instability*, takes this into account by alluding to the need for contact with another entity, the current system of an auroral streamer bubble or the like.

An interesting question is whether the observed bead motion is a phase propagation or a convective flow. The way we have discussed above, the density perturbations propagate by the two forces joining to push

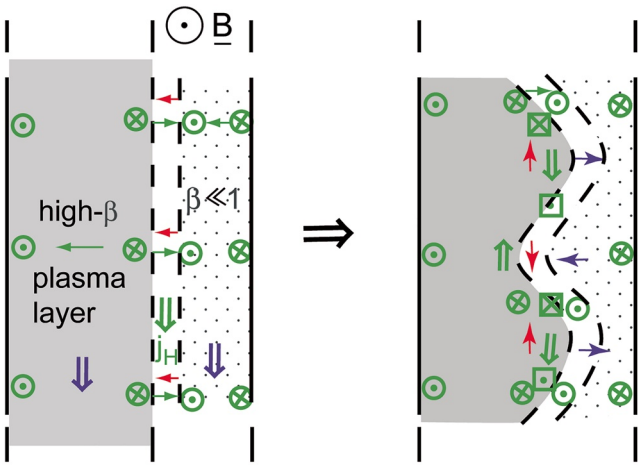


**Figure 8.** (a) Currents, fields, and flows in the equatorial plane at beginning of current sheet mating by ion currents crossing the gap between growth phase arc and new arc. (b) Onset of beading instability.

the plasma not only inward and outward, but from the outset also in longitude. The generated kinetic Alfvén waves transport energy and momentum earthward. However, the feedback from the ionosphere is not as strong as with quasi-stationary Alfvén waves, like in the fascinating evening arcs. Haerendel and Frey (2014) found that kinetic Alfvén waves at the poleward border of the auroral oval were largely decoupled from the frictional ionosphere, in agreement with the loss of Poynting flux along B found by Wygant et al. (2000) and Keiling et al. (2009). However, some longitudinal momentum must be imparted to the immediate environment. This constitutes a drag force on the generator plasma. We, therefore, conclude that the bead motion is a convective motion with little ionospheric control.

Nevertheless, the longitudinal motions raise the question of momentum and magnetic flux conservation. The longitudinal momentum balance has to do with the shear stresses established by the convection inside the GPA. For instance, on the evening side, displayed in Figure 7, the high-beta plasma has been pushed westward by pressure forces during the growth phase. These forces were balanced by opposing shear stresses. As the mating instability proceeds, the involved plasma loses internal energy, the pressure is reduced, and opposing magnetic shear stresses can act as generator forces in the direction of the bead motion.

Although the kinetic Alfvén waves at least partially decoupled from the ionosphere (Haerendel & Frey, 2014), the bead flow constitutes a transport of magnetic field in longitude. Closer to Earth, the incompressibility of the magnetic field demands the existence of a return flow. It may be turbulent, but on average opposite to the bead motion and located in the flow channel of the streamer bubble. The lower ionospheric conductivity poleward of the GPA, enhanced by decoupling in the topside ionosphere, allows a fast return flow. This return flow has not yet been directly observed, but fast ray motions, seen in the video of the March 1, 2011 event (Supporting Information 1), support this supposition. What this means in essence is, that for the instability of the high-beta plasma the mating of the two adjacent current sheets is not sufficient. It needs the involvement of an opposing flow channel. This is offered by the balanced current system of the new arc in the first event or the streamer in the second. For this reason, the hot plasma remains stable until contact with such a configuration is established.

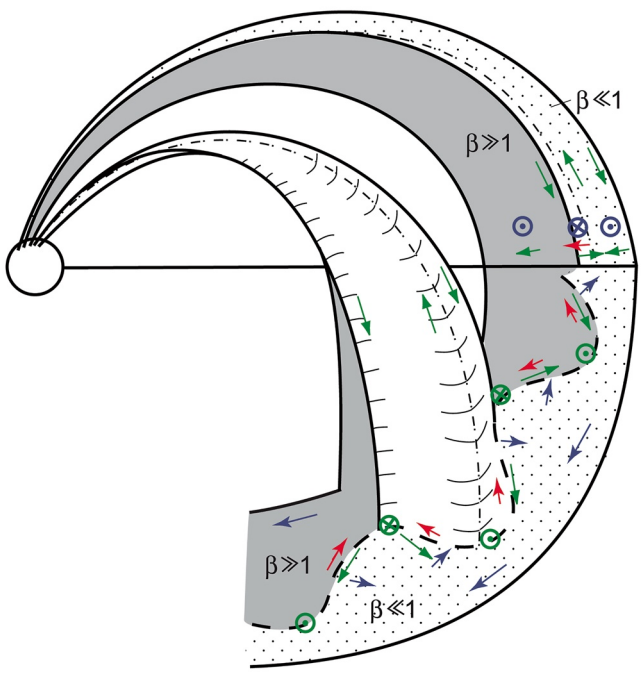


**Figure 9.** View of the high-beta plasma layer with beads, shown in meridian and equatorial projections for an evening situation. One selected protrusion is shown with its extension toward the ionosphere. Currents (green arrows), sources and sinks of field-aligned currents (green circles).

The sequence of events at March 1, 2011 substorm onset leads to some difficult questions. We observe that the critical narrow gap is not created by the E-W arc lining up with the GPA, but with a new arc closer to the GPA. Closer inspection shows that it is not coincident with the diffuse arc seen already 6 min earlier in the gap with the E-W arc. The bright rays emerging from the visible eastern edge, brightening and moving quickly westward appear even closer to the GPA, miraculously just at the time of beading onset. The westward progression of the rays is more or less synchronous with the spreading of the brightening of the beads. So we have to ask ourselves: Does the proposed mating of current sheets proceed with an existing close arc or is it newly created by the instability? If the latter were the case, one would have to wonder why this did not happen much earlier, why the onset had to wait for the arrival of the E-W arc and the new arc forming in the gap. More convincing is the explanation that the previously existing westward flow inside the mating arc is activated for housing the above-discussed return flow. Unfortunately, Whitehorse, the closest all-sky camera to the east of Poker Flat/Gakona, did not produce images at all. Farther east, at Fort Simpson, one just sees the GPA

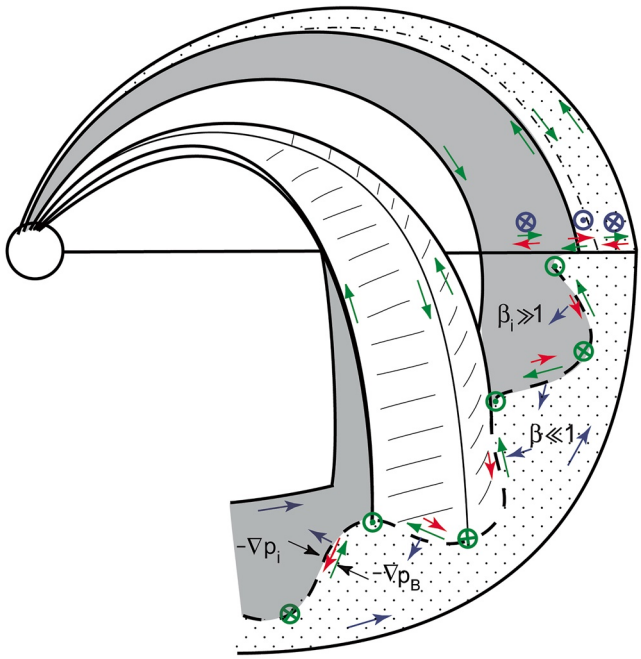


**Figure 10.** Same as Figure 9 for the morning situation. At the left edge, the force balance between new arc and growth phase arc is shown.

moving equatorward. The subsequent substorm appears many minutes delayed. Very clearly, the substorm onset was centered above Gakona. We have no insight into the happenings outside the FoV of the cameras that delivered our data set. Aspect angles and spatial resolution of our second event (February 29, 2008) do not allow at all a detailed analysis of the kind presented above. The hope remains that eventually, numerical simulations will allow tackling these and other questions posed by the proposed mating instability.

All of the above was derived from the analysis of two well-resolved onset events. The question is whether the proposed mating process can be generalized to any triggering of the brightening and instability of the onset arc. If this were the case, how could we reconcile the appearance of opposing bead flows with the observations of Nishimura et al. (2016), which would imply that the beads should move in the *same* direction as the convective flow inside the GPA? In spite of the large scatter of the underlying data, there is a conflict, which cannot be solved without turning to other, well-resolved onset events. There is perhaps a hint coming from our morning-side event. After a short while of westward motions, the chain of beads was splitting, with the eastern part moving eastward. However, this may have been an effect of the arriving flow bursts. At this point, we must be content with having presented, for the first time, a plasma physical mechanism for the triggering of a ballooning instability of the high-beta plasma layer above the GPA.

## 7. Summary

We have addressed the problem of substorm onset in five steps.

**Step 1** : With analyzing one well-documented event, we underpin the statement that brightening of the onset arc with beading is independent of reconnection in the tail and flow burst ejection. Both processes are owed to extreme thinning of the tail current sheet during the growth phase.

**Step 2** : The energy source of the nonlinear beading instability is a layer of high-beta plasma building up during the growth phase by accumulation and compression of plasma from the tail plasma sheet toward and along the outer boundary of the near-dipolar magnetosphere.

**Step 3** : After summarizing what is known about the nature of auroral streamers, we conclude that there may be two classes distinguished by their electron spectra and their optical appearance. High time-resolution imaging of the rayed structure of pre-onset E-W arcs suggest that they must be Alfvénic arcs. From their fast propagation and attachment with flow channels, we conclude that the overarching structure of a streamer may be that of a low-entropy content bubble. However, there are some open questions.

**Step 4** : The magnitude and the systematics of observed bead motions in relation to the convection velocities inside and poleward of the growth phase arc, lead to the conclusion that the bead motion must be intrinsic to the instability process. Close inspection of two high-resolution onset events along the evening GPA reveals that the beads form in the gap between the high-beta plasma and the flux tube above the auroral streamer. However, in one of the two events, it is the appearance of a new arc between the E-W arc and the GPA that is actually creating an even narrower gap with the latter. The intriguing fact that the direction of bead motion is opposed to the flow directions on either side of the gap leads us to propose that the basic process is a non-MHD process allowing the *mating* between the two neighboring current sheets by a bridging current. Like in the collision-free reconnection, charge neutrality requires continuation by field-aligned currents and electric fields driving Hall currents. Perturbations of the density contours act as sources and sinks of such currents. Small-scale e.m. fields appear enabling growth of the perturbations. The generator property of the bridging currents is likely to determine the sense of electric fields consistent with

the observed bead motions. Since the key to the ensuing instability is the mating of two, previously independent current sheets, we designate it as *mating instability*.

**Step 5** : The basic situation of the mating instability is an equilibrium between the plasma pressure on the side of the GPA and the enhanced magnetic pressure of the new arc. When the equilibrium is disturbed by the onset of the mating current, perturbations can grow. Their nonlinear evolution is either dominated by the force from the side of the high-beta plasma or that of the new arc. The winner is the force acting from the side of the emerging upward current. On the evening side, it is the plasma pressure force; therefore, perturbations grow poleward. On the morning side, it is the magnetic pressure force; therefore, perturbations grow earthward. This is actually observed in the two analyzed events. The two forces join in driving the perturbations in longitude. The direction is determined by the sense of the dominant bridging currents. The deeper lying reason lies in the release of shear stresses present in the growth phase arc when the plasma pressure in the mating process is reduced by the shedding of internal energy. Perturbations of the longitudinal ion pressure profile act as sources of kinetic Alfvén waves, which are the origin of the beads. Their overall role is to transport internal energy expended by the high-beta plasma and momentum from the winning force downwards to the ionosphere. Furthermore, the incompressibility of the near-Earth magnetic field requires the existence of a counter-flow to that of the beads, which in our scenario is a flow rather than a wave motion. The counter-flow must be located in the flow channel of the streamer bubble.

In short, we can say: In searching for a trigger of the nonlinear beading instability, we have come across an entirely new non-MHD process, the mating of neighboring current sheets, leading to the formation of a new balanced current system that readily breaks into small-scale Alfvénic structures transporting free energy toward the ionosphere. Since the above has been deduced from the analysis of only two events, it has to be seen whether the mating instability is underlying all beading events or whether there are alternate processes. In any case, beading may accompany a substorm onset but certainly does not cause it.

## Data Availability Statement

In particular, the authors thank S. Mende and E. Donovan for use of the ASI data, the CSA for logistical support in fielding and data retrieval from the GBO stations, and S. Mende and C. T. Russell for use of the GMAG data. The all sky video of Joshua L. Semeter and Don Hampton (Boston University) has been of great help for the analysis of Event #1. We are most grateful for the permission to use the information in the text and Supporting Information 1. The authors are indebted to the FAST science team, especially J. McFadden and R. Strangeway, for the use of FAST data in Figure A1. THEMIS ASI and GMAG data are publicly available through the THEMIS data repository at http://themis.ssl.berkeley.edu/data/themis/. The SPEDAS software suite (Angelopoulos et al., Space Science Reviews, 215:9, https://doi.org/10.1007/s11214-018-0576-4, 2019) can be used to retrieve, display, manipulate, and analyze THEMIS data. The FAST data are available through the NASA Space Physics Data Facility (SPDF) at https://spdf.gsfc.nasa.gov/.

**Acknowledgments**
One of the authors (G.H.) is greatly indebted to Dr. Richard (Dick) Wolf for intensive discussions of the theoretical foundations of the subject of this manuscript. We acknowledge NASA contract NAS5-02099 and V. Angelopoulos for use of data from the THEMIS Mission. Open access funding enabled and organized by Projekt DEAL.

## References

Akasofu, S.-I. (1964). The development of the auroral substorm. *Planetary and Spac Sciences*, *12*, 273–282. https://doi.org/10.1016/0032-0633(64)90151-5

Angelopoulos, V., McFadden, J. P., Larson, D., Carlson, C. W., Mende, S. B., Frey, H., et al. (2008). Tail reconnection triggering substorm onset. *Science*, *321*, 931–935. https://doi.org/10.1126/science.1160495

Arnoldy, R. L., Lynch, K. A., Austin, J. B., & Kintner, P. M. (1999). Energy and pitch angle- dispersed auroral electrons suggesting a time-variable, inverted-V potential structure. *Journal of Geophysical Research*, *104*(22), 22613–22621. https://doi.org/10.1029/1999JA900219

Baumjohann, W., Paschmann, G., & Catell, C. A. (1989). Average plasma properties in the central plasma sheet. *Journal of Geophysical Research*, *94*, 6597–6606. https://doi.org/10.1029/JA094iA06p06597

Baumjohann, W., Pellinen, R. J., Opgenoorth, H. J., & Nielsen, E. (1981). Joint two-dimensional observations of ground magnetic and ionospheric electric fields associated with auroral zone currents: Current systems associated with local auroral break-ups. *Planetary and Space Sciences*, *29*(No. 4), 431–447. https://doi.org/10.1016/0032-0633(81)90087-8

Birn, J., & Hesse, M. (2013). The substorm current wedge in MHD simulations. *Journal of Geophysical Research*, *118*, 3364–3376. https://doi.org/10.1002/jgra.5550187

Birn, J., Hesse, M., Haerendel, G., Baumjohann, W., & Shiokawa, K. (1999). Flow braking and the substorm current wedge. *Journal of Geophysical Research*, *104*(19), 19895–19903. https://doi.org/10.1029/1999ja900173

Birn, J., Raeder, J., Wang, Y. L., Wolf, R. A., & Hesse, M. (2004). On the propagation of bubbles in the geomagnetic tail. *Annals of Geophysics*, *22*, 1773–1786. https://doi.org/10.5194/angeo-22-1773-2004

Chaston, C. C., Carlson, C. W., Ergun, R. E., McFadden, J. P., & Strangeway, R. J. (2003). Properties of small-scale Alfvén waves and accelerated electrons from FAST. *Journal of Geophysical Research*, *108*(A4), 8003. https://doi.org/10.1029/2002JA009420
Chaston, C. C., Gernot, V., Bonnell, J. W., Carlson, C. W., McFadden, J. P., Ergun, R. E., et al. (2006). Ionospheric erosion by Alfvén waves. *Journal of Geophysical Research*, *111*, A03206. https://doi.org/10.1029/2005ja011367
Chaston, C. C., Salem, C., Bonnell, J. W., Carlson, C. W., Ergun, R. E., Strangeway, R. J., & McFadden, J. P. (2008). The turbulent Alfvénic aurora. *Physical Review Letters*, *100*, 175003. https://doi.org/10.1103/physrevlett.100.175003
Chen, C.-X., & Wolf, R. A. (1993). Interpretation of high speed flows in the plasma sheet. *Journal of Geophysical Research*, *98*(21), 409–21419. https://doi.org/10.1029/93JA02080
Coroniti, F. V., & Kennel, C. F. (1972). Can the ionosphere regulate ionospheric flow? *Journal of Geophysical Research*, *78*, 2837–2851. https://doi.org/10.1029/JA078i016p02837
Coroniti, F. V., & Pritchett, P. L. (2014). The quiet evening auroral arc and the structure of the growth phase rear-Earth plasma sheet. *Journal of Geophysical Research Space Physics*, *119*, 1827–1836. https://doi.org/10.1002/2013JA019435
Dahlgren, H., Semeter, J. L., Marshall, R. A., & Zettergren, M. (2013). The optical manifestation of dispersive field-aligned bursts in auroral breakup arcs. *Journal of Geophysical Research*, *118*, 4572–4582. https://doi.org/10.1002/jgra.50415
Deehr, C., & Lummerzheim, D. (2001). Ground-based optical observations of hydrogen emission in the auroral substorm. *Journal of Geophysical Research*, *106*(A1), 33–44. https://doi.org/10.1029/2000ja002010
Derr, J., Horton, W., & Wolf, R. (2020). Shear-flow-interchange instability in nightside magnetotail causes auroral beads as a signature of substorm onset. *Journal of Geophysical Research*, *125*. https://doi.org/10.1029/2019JA026885
Donovan, E., Mende, S., Jackel, B., Frey, H., Syrjäsuo, M., Voronkov, I., et al. (2006). The THEMIS all-sky imaging array – System design and initial results from the prototype imager. *Journal of Atmospheric and Solar Terrestrial Physics*, *68*, 1472–1487. https://doi.org/10.1016/j.jastp.2005.03.027
Dubyagin, S. V., Sergeev, V. A., Carlson, C. W., Marple, S. R., Pulkkinen, T. I., & Yahnin, A. G. (2003). Evidence of near-Earth breakup location. *Geophysical Research Letters*, *30*, 1282. https://doi.org/10.1029/2002GL016569
Elphinstone, R. D., Hearn, D. J., Cogger, L. L., Murphree, J. S., Singer, H., Sergeev, V., et al. (1995). Observation in the vicinity of substorm onset: Implications for the substorm process. *Journal of Geophysical Research*, *100*, 7937–7979. https://doi.org/10.1029/94JA02938
Forsyth, C., Sergeev, V. A., Henderson, M. G., Nishimura, Y., & Gallardo-Lacourt, B. (2020). Physical processes of meso-scale, dynamic auroral forms. *Space Science Reviews*, *216*, 46. https://doi.org/10.1007/s11214-20-00665-y
Frey, H. U., Haerendel, G., Knudsen, D., Buchert, S., & Bauer, O. H. (1996). Optical and radar observations of the motion of auroral arcs. *Journal of Atmospheric and Terrestrial Physics*, *58*, 57–69. https://doi.org/10.1016/0021-9169(95)00019-4
Gallardo-Lacourt, B., Nishimura, Y., Lyons, L. R., Zou, S., Angelopoulos, V., Donovan, E., et al. (2014). Coordinate SuperDARN THEMIS ASI observations of mesoscale flow bursts associated with auroral streamers. *Journal of Geophysical Research*, *119*, 142–150. https://doi.org/10.1002/2013JA019245
Haerendel, G. (2010). Equatorward moving arcs and substorm onset. *Journal of Geophysical Research*, *115*, A07212. https://doi.org/10.1029/2009JA015117
Haerendel, G. (2015a). Substorm onset: Current sheet avalanche and stop layer. *Journal of Geophysical Research*, *120*. https://doi.org/10.1002/2014JA020571
Haerendel, G. (2015b). Flow bursts, breakup arc, and substorm current wedge. *Journal of Geophysical Research*, *120*, 2796–2807. https://doi.org/10.1002/2014JA020954
Haerendel, G., Buchert, S., LaHoz, C., Raaf, B., & Rieger, E. (1993). On the proper motion of auroral arcs. *Journal of Geophysical Research*, *98*, 6087–6099. https://doi.org/10.1029/92ja02701
Haerendel, G., & Frey, H. U. (2014). Role and origin of the poleward Alfvénic arc. *Journal of Geophysical Research: Space Physics*, *119*, 2945–2962. https://doi.org/10.1002/2014JA019786
Haerendel, G., Frey, H. U., chaston, C. C., Amm, O., Juusola, L., Nakamura, R., et al. (2012). Birth and life of auroral arcs embedded in the evening auroral oval convection: A critical comparison of observations wth theory. *Journal of Geophysical Research*, *117*, A12220–n. https://doi.org/10.1029/2012JA018128
Henderson, M. G., Murphree, J. S., & Reeves, G. D. (1994). The activation of the dusk-side and the formation of north-south aligned structures during substorms. In J. R. Kan, J. D. Craven, S.-I. Akasofu, & p. (Eds.), *Proceedings of the second International Conference on substorms* (p. 37.): Univ. of Alaska Fairbanks.
Ivchenko, N., Marklund, G., Lynch, K., Pietrowski, D., Torbert, R., Primdahl, F., & Ranta, A. (1999). Quasiperiodic oscillations observed at the edge of an auroral arc by Auroral Turbulence 2. *Geophysical Research Letters*, *26*, 3365–3368. https://doi.org/10.1029/1999GL003588
Kadokura, A., Yukimatu, A.-S., Ejiri, M., Oguti, T., Pinnock, M., & Hairston, M. R. (2002). Detailed analysis of a substorm event on 6 and 7 June 1989, 1, Growth phase evolution of nightside auroral activities and ionospheric convection toward expansion phase onset. *Journal of Geophysical Research*, *107*(A12), 1479–1481. https://doi.org/10.1029/2001JA009127
Kalmoni, N. M. E., Rae, I. J., Murphy, K. R., Forsyth, C., Watt, C. E. J., & Owen, C. J. (2017). Statistical azimuthal structuring of the substorm onset arc: Implications for the onset mechanism. *Geophysical Research Letters*, *44*, 2078–2087. https://doi.org/10.1002/2016GL071826
Kalmoni, N. M. E., Rae, I. J., Watt, C. E. J., Murphy, K. R., Forsyth, C., & Owen, C. J. (2015). Statistical characterization of the growth and spatial scales of the substorm onset arc. *Journal of Geophysical Research*, *120*, 8503–8516. https://doi.org/10.1002/2015JA021470
Kalmoni, N. M. E., Rae, I. J., Watt, C. E. J., Murphy, K. R., Samara, M., Mitchell, R. G., et al. (2018). A diagnosis of the plasma waves responsible for the explosive energy release of substorm onset. *Nature Communications*, *9*, 4806. https://doi.org/10.1038/s41467-018-07086-0
Kataoka, R., Miyoshi, Y., Sakanoi, T., Yaegashi, A., Shiokawa, K., & Ebihara, Y. (2011). Turbulent microstructures and formation of folds in auroral breakup arc. *Journal of Geophysical Research*, *116*, A00K02. https://doi.org/10.1029/2010JA016334
Kauristie, K., Sergeev, V. A., Kubyshkina, M., Pulkkinen, T. I., Angelopoulos, V., Phan, T., et al. (2000). Ionospheric current signatures of transient plasma flows. *Journal of Geophysical Research*, *105*(10), 677–710. https://doi.org/10.1029/1999ja900487
Keiling, A. (2009). Alfven waves and their roles in the dynamics of the Earth's magnetotail: A review. *Space Science Reviews*, *142*(1–4), 73–156. https://doi.org/10.1007/s11214-008-9463-8
Kornilova, T. A., Kornilov, I. A., & Kornilov, O. I. (2006). Auroral intensification structure and dynamics in the auroral oval: Substorm of December 26, 2000. *Geomagnetism and Aeronomy*, *46*, 450–456. https://doi.org/10.1134/S0016793206040062
Liang, J., Donovan, E. F., Sofko, G. J., & Trondsen, T. (2005). Substorm dynamics revealed by ground observations of two-dimensional auroral structures on 9 October 2000. *Annals of Geophysics*, *23*, 3599–3613. https://doi.org/10.5194/angeo-23-3599-2005
Louarn, P., Wahlund, J.-E., Chust, T., de Feraudy, H., Roux, A., Holback, B., et al. (1994). Observations of kinetic Alfvén waves by the Freja spacecraft. *Geophysical Research Letters*, *21*, 1847–1850. https://doi.org/10.1029/94GL00882

Lui, A. T. Y. (1991). A synthesis of magnetospheric substorm models. *Journal of Geophysical Research*, *96*(A2), 1849–1856. https://doi.org/10.1029/90JA02430
Lui, A. T. Y. (2020). Evaluation of the cross-field current instability as a substorm onset process with aurora lead properties. *Journal of Geophysical Research: Space Physics*, *125*, e2020JA027867. https://doi.org/10.1029/2020/JA0222227867
Lui, A. T. Y., & Hamilton, D. C. (1992). Radial profiles of quiet time magnetospheric parameters. *Journal of Geophysical Research*, *97*(19), 325–332. https://doi.org/10.1029/92JA01539
Lui, A. T. Y., Mankovsky, A., Chang, C.-L., Papadopoulos, K., & Wu, C. S. (1990). A current disruption mechanism in the neutral sheet: A possible trigger for substorm expansions. *Geophysical Research Letters*, *17*(6), 745–748. https://doi.org/10.1029/GL017i006p00745
Lyons, L. R., Voronkov, I. O., Donovan, E. F., & Zesta, E. (2002). Relation of substorm breakup arc to other growth-phase auroral arcs. *Journal of Geophysical Research*, *107*, A11. https://doi.org/10.1029/2002JA009317
Mende, S., Angelopoulos, V., Frey, H. U., Donovan, E., Jackel, B., Glassmeier, K.-H., et al. (2009). Timing and location of substorm onsets from THEMIS satellite and ground based observations. *Annals of Geophysics*, *27*, 2813–2830. https://doi.org/10.5194/angeo-27-2813-2009
Mende, S. B., carlson, C. W., Frey, H. U., Peticolas, L. M., & Ostgaard, N. (2003). FAST and IMAGE-FUV observations of a substorm onset. *Journal of Geophysical Research*, *108*, 1344. https://doi.org/10.1029/2002JA009787
Mende, S. B., Frey, H. U., Angelopoulos, V., & Nishimura, Y. (2011). Substorm triggering by poleward boundary intensification and related equatorward propagation. *Journal of Geophysical Research*, *116*, A00131. https://doi.org/10.11029/2010JA015733
Nakamura, R., Baumjohann, W., Schödel, R., Brittnacher, M., Sergeev, V. A., Kubyshkina, M., et al. (2001). Earthward flow bursts, auroral streamers, and small expansions. *Journal of Geophysical Research*, *106*(A6), 791–810. https://doi.org/10.1029/2000ja000306
Nakamura, R., Oguti, T., Yamamoto, T., & Kokobun, S. (1993). Equatorward and poleward expansion and the auroras during auroral substorms. *Journal of Geophysical Research*, *98*, 5743–5759. https://doi.org/10.1029/92JA02230
Newell, P. T., et al. (1996). Morphology of nightside precipitation. *Journal of Geophysical Research*, *101*(10), 737. https://doi.org/10.1029/95ja03516
Nishimura, Y., Lyons, L., Zou, S., Angelopoulos, V., & Mende, S. (2010). Substorm triggering by new plasma intrusion: THEMIS all-sky imager observations. *Journal of Geophysical Research*, *115*, A07222. https://doi.org/10.1029/2009JA015166
Nishimura, Y., Lyons, L. R., Nicolls, M. J., Hampton, D. L., Michell, R. G., Samara, M., et al. (2014). Coordinated ionospheric observations indicating coupling between preonset flow bursts and waves that lead to substorm onset. *Journal of Geophysical Research*, *119*, 3333–3344. https://doi.org/10.1002/2014JA019773
Nishimura, Y., Yang, J., Pritchett, P. L., Coroniti, F. V., Donovan, E. F., Lyons, L. R., et al. (2016). Statistical properties of substorm auroral onset beads/rays. *Journal of Geophysical Research*, *121*, 8661–8676. https://doi.org/10.1002/2016JA022801
Oguti, T. (1973). Hydrogen emission and electron aurora at the onset of the auroral breakup. *Journal of Geophysical Research*, *78*, 7543–7547. https://doi.org/10.1029/ja078i031p07543
Ohtani, S. I., & Tamao, T. (1993). Does the ballooning instability trigger substorms in the near-Earth magnetotail? *Journal of Geophysical Research*, *98*, 19–369. https://doi.org/10.1029/93ja01746
Pellinen, R. J., & Heikkila, W. J. (1978). Observations of auroral fading before breakup. *Journal of Geophysical Research*, *83*(A9), 4207–4217. https://doi.org/10.1029/ja083ia09p04207
Pontius, D. H., Jr, & Wolf, R. A. (1990). Transient flux tubes in the terrestrial magnetosphere. *Geophysical Research Letters*, *17*, 49–52. https://doi.org/10.1029/gl017i001p00049
Pritchett, P. L., & Coroniti, F. V. (2010). Plasma sheet disruption by interchange-generated flow intrusions. *Geophysical Research Letters*, *38*, L10102. https://doi.org/10.1029/2011GL047527
Rae, I. J., Mann, I. R., Murphy, K. R., Milling, D. K., Parent, A., Angelopoulos, V., et al. (2009). Near-Earth initiation of terrestrial substorm onset. *Journal of Geophysical Research*, *114*, A00C09. https://doi.org/10.1029/2008JA013559
Rostoker, G., Lui, A. T. Y., Anger, C. D., & Murphree, J. S. (1987). North-south structures in the midnight sector auroras as viewed by the Viking imager. *Geophysical Research Letters*, *14*, 407–410. https://doi.org/10.1029/GL014i004p00407
Roux, A., Perraut, S., Robert, P., Morane, A.,Pedersen, A., Korth, A., et al. (1991). Plasma sheet instability related to the westward traveling surge. *Journal of Geophysical Research*, *96*(A10), 17697–17717. https://doi.org/10.1029/91ja01106
Runov, A., Angelopoulos, V., Sitnov, M. I., Sergeev, V. A., Bonnell, J., McFadden, J. P., et al. (2009). THEMIS observations on an earthward-propagating dipolarization front. *Geophysical Research Letters*, *36*. https://doi.org/10.1029/2009GL038980
Sakaguchi, K., Shiokawa, K., Ieda, A., Nomura, R., Nakajima, A., Greffen, M., et al. (2009). Fine structures and dynamics in auroral initial brightening at substorm onsets. *Annals of Geophysics*, *27*, 623–630. https://doi.org/10.5194/angeo-27-623-2009
Samson, J. C., Lyons, L. R., Newell, P. T., Creutzberg, F., & Xu, B. (1992). Proton aurora and substorm intensifications. *Geophysical Research Letters*, *19*(No. 21), 2167–2170. https://doi.org/10.1029/92gl02184
Sergeev, V., Angelopoulos, V., Kubyshkina, M., Donovan, E., Zhou, X.-Z., Runov, A., et al. (2011). Substorm growth and expansion onset as observed with ideal ground-spacecraft THEMIS coverage. *Journal of Geophysical Research*, *116*, A00126. https://doi.org/10.1029/2010JA015689
Sergeev, V. A., Angelopoulos, V., & Nakamura, R. (2012). Recent advances inunderstanding substorm dynamics. *Geophysical Research Letters*, *39*, L05101. https://doi.org/10.1029/2012GL050859
Sergeev, V. A., Sauvaud, J.-A., Popesco, D., Kovrazkhin, R. A., Lutsenko, V. N., Zelenyi, L. M., et al. (2000). Plasma sheet ion injections into the auroral bulge: Correlative study of spacecraft and ground observations. *Journal of Geophysical Research*, *105*(A8), 18465–18518. https://doi.org/10.1029/1999ja900435
Sergeev, V. A., Liou, K., Newell, P. T., Ohtani, S.-I., Hairston, M. R., & Rich, F. (2004). Auroral streamers: Characterisctics of associated precipitation, convection and field-aligned currents. *Annals of Geophysics*, *22*, 537–548. https://doi.org/10.5194/angeo-22-537-2004
Sergeev, V. A., Malkov, M. V., & Mursula, K. (1993). Testing the isotropic boundary algorithm method to evaluate the magnetic field configuration in the tail. *Journal of Geophysical Research*, *98*, 7609–7620. https://doi.org/10.1029/92ja02587
Shiokawa, K., Baumjohann, W., & Haerendel, G. (1997). Braking of high-speed flows in the near-Earth tail. *Geophysical Research Letters*, *24*, 1179–1182. https://doi.org/10.1029/97gl01062
Shiokawa, K., Ieda, A., Nakajima, A., Sakaguchi, K., Nomura, R., Aslaksen, T., et al. (2009). Longitudinal development of a substorm brightening arc. *Annals of Geophysics*, *27*, 1935–1940. https://doi.org/10.5194/angeo-27-1935-2009
Sorathia, K. A., Merkin, V. G., Panov, E. V., Zhang, B., Lyon, J. G., Garretson, J., et al. (2020). Ballooning-interchange instability in the near Earth plasma sheet and auroral beads: Global magnetospheric modelling at the limit of the MHD approximation. *Geophysical Research Letters*, *47*, e2020GL088227. https://doi.org/10.1029/2020gl088227
Stasiewicz, K., Bellan, P., Chaston, C., Kletzing, C., Lysak, R., Maggs, J., et al. (2000). Small scale Alfvenic structure in the aurora. *Space Science Reviews*, *92*, 423–533. https://doi.org/10.1023/a:1005207202143

Voronkov, I., Rankin, R., Frycz, P., Tikhonchuk, V. T., & Samson, J. C. (1997). Coupling of shear flow and pressure gradient instabilities. *Journal of Geophysical Research*, *102*(A5), 9639–9650. https://doi.org/10.1029/97ja00386

Wahlund, J.-E., Louarn, P., Chust, T., de Feraudy, H., Roux, A., Holback, B., et al. (1994).. *Geophysical Research Letters*, *21*(No. 17), 1831–1834. https://doi.org/10.1029/94gl01289

Wygant, J. R., Keiling, A., Cattell, C. A., Johnson, M., Lysak, R. L., Temerin, M., et al. (2000). Polar spacecraft based comparisons of intense electric fields and Poynting flux near and within the plasma sheet tail lobe boundary to UV images: An energy source of the aurora. *Journal of Geophysical Research*, *105*(18), 675–692. https://doi.org/10.1029/1999JA900500

Yang, J., Toffoletto, F. R., & Wolf, R. A. (2014). RCM-E simulation of a thin arc preceded by a north-south aligned auroral streamer. *Geophysical Research Letters*, *41*, 2695–2701. https://doi.org/10.1002/2014GL059840

Yang, J., Wolf, R. A., Toffoletto, F. R., & Sazykin, S. (2013). RCM-E simulation of substorm growth phase arc associated with large-scale adiabatic convection. *Geophysical Research Letters*, *40*, 6017–6022. https://doi.org/10.1002/2013GL058253

Zesta, E., Donovan, E., Lyons, L., Enno, G., Murphree, J. S., & Cogger, L. (2002). Two-dimensional structure of auroral poleward boundary intensifications. *Journal of Geophysical Research*, *107*, A11. https://doi.org/10.1029/2001JA000260